Journal of Cellular Biochemistry 103:1144–1157 (2008)

Methylglyoxal and High Glucose Co-Treatment Induces Apoptosis or Necrosis in Human Umbilical Vein Endothelial Cells

Wen-Hsiung Chan[1,2]* and Hsin-Jung Wu[1]

[1]Department of Bioscience Technology and Center for Nanotechnology, Chung Yuan Christian University, Chung Li, Taiwan
[2]R&D Center for Membrane Technology, Chung Yuan Christian University, Taiwan

Abstract Hyperglycemia and elevation of methylglyoxal (MG) are symptoms of diabetes mellitus (DM). We previously showed that high glucose (HG; 30 mM) or MG (50–400 μM) could induce apoptosis in mammalian cells, but these doses are higher than the physiological concentrations of glucose and MG in the plasma of DM patients. The physiological concentration of MG and glucose in the normal blood circulation is about 1 μM and 5 mM, respectively. Here, we show that co-treatment with concentrations of MG and glucose comparable to those seen in the blood circulation of DM patients (5 μM and 15–30 mM, respectively) could cause cell apoptosis or necrosis in human umbilical vein endothelial cells (HUVECs) in vitro. HG/MG co-treatment directly increased the reactive oxygen species (ROS) content in HUVECs, leading to increases in intracellular ATP levels, which can control cell death through apoptosis or necrosis. Co-treatment of HUVECs with 5 μM MG and 20 mM glucose significantly increased cytoplasmic free calcium levels, activation of nitric oxide synthase (NOS), caspase-3 and -9, cytochrome *c* release, and apoptotic cell death. In contrast, these apoptotic biochemical changes were not detected in HUVECs treated with 5 μM MG and 30 mM glucose, which appeared to undergo necrosis. Pretreatment with nitric oxide (NO) scavengers could inhibit 5 μM MG/20 mM glucose-induced cytochrome *c* release, decrease activation of caspase-9 and caspase-3, and increase the gene expression and protein levels of p53 and p21, which are known to be involved in apoptotic signaling. Inhibition of p53 protein expression using small interfering RNA (siRNA) blocked the activation of p21 and the cell apoptosis induced by 5 μM MG/20 mM glucose. In contrast, inhibition of p21 protein expression by siRNA prevented apoptosis in HUVECs but had no effect on p53 expression. These results collectively suggest that the treatment dosage of MG and glucose could determine the mode of cell death (apoptosis vs. necrosis) in HUVECs, and both ROS and NO played important roles in MG/HG-induced apoptosis of these cells. J. Cell. Biochem. 103: 1144–1157, 2008.

Key words: high glucose; methylglyoxal; apoptosis; necrosis; ROS; nitric oxide

Hyperglycemia and increased methylglyoxal (MG) levels, two major symptoms seen in DM patients, can have long-term effects on blood cells and the endothelial cells of blood vessels [Okado et al., 1996; Ho et al., 2000]. Recent reports have shown that the hyperosmotic environment created by hyperglycemia can cause various cell injuries, including apoptosis [Ho et al., 2000; Chan, 2005]. HG-induced cell apoptosis has been shown to be mediated by oxidative stress and JNK activation [Ho et al., 2000; Chan, 2005], and cell responses triggered by high levels of MG have been studied in several mammalian cell types [Chan et al., 2005; Hsuuw et al., 2005]. However, the combined effects of MG and hyperglycemia in blood, and the signaling pathways underlying these possible effects, have not yet been studied in detail.

High glucose treatment induces a hyperosmotic shock environment, leading to osmotic stress, which triggers various cell responses, including apoptosis [Qin et al., 1997; Chan et al., 1999; Chan, 2005]. Our previous study showed

Grant sponsor: National Science Council of Taiwan, ROC; Grant numbers: 95-2311-B-033-001-MY3, NSC 95-2627-M-033-004.

*Correspondence to: Wen-Hsiung Chan, Department of Bioscience Technology and Center for Nanotechnology, Chung Yuan Christian University, Chung Li 32023, Taiwan. E-mail: whchan@cycu.edu.tw

Received 2 April 2007; Accepted 18 June 2007

DOI 10.1002/jcb.21489

that hyperosmotic shock induced cell apoptosis through multiple biochemical changes, including ROS generation, activation of JNK and caspase-3, and DNA fragmentation. We further found that these effects could be blocked by antioxidants, suggesting that ROS play important roles in hyperglycemia-induced cell apoptosis [Chan, 2005]. However, the effects of the hyperglycemic environment on blood cells and blood vessel endothelial cells have not yet been evaluated.

MG is a reactive dicarbonyl compound that is formed as a metabolic byproduct of glycolysis, and is also produced in various foodstuffs during processing, including freshly brewed coffee and soy sauce [Kasai et al., 1982]. Coffee is highly consumed throughout the world and the intake of MG by drinking 2–3 cups of coffee can be calculated to be as much as 1 mg/day [Kasai et al., 1982]. For the general population, the MG concentration in blood is approximately 1 μM, while diabetics have 3–6 times that amount [McLellan et al., 1994], and levels in diabetics can remain elevated for several months and even years. MG is often found at high levels in the blood of diabetic patients, leading to serious toxicological effects. MG can cross-link with the amino groups of various proteins, forming stable end products called advanced glycation end products (AGEs) [Brownlee et al., 1988; Bourajjaj et al., 2003]. Because diabetic complications develop at a slow rate, the long term effect of MG on the formation of AGEs has been well investigated [Shipanova et al., 1997; Uchida et al., 1997]. In addition, MG may modify cross-linked lysine and arginine residues, altering the protein characteristics and producing reactive oxygen species (ROS) during the glycation reaction [Yim et al., 1995; Chan and Wu, 2006; Wu and Chan, 2006, 2007]. Oxidative stress and AGE formation have been associated with impaired cognitive processes in diabetic patients [Messier and Gagnon, 1996; Gerozissis, 2003], suggesting that this may be linked to MG toxicity. Recently, several studies have showed that MG can induced cell apoptosis in several cell lines including Schwann cells, PC-12 cells, and renal tubular cells [Jan et al., 2005; Okouchi et al., 2005; Ota et al., 2007]. However, the cytotoxic effects and regulatory mechanisms of MG on endothelial cells are unclear and need further investigation.

Numerous chemical and physical treatments capable of inducing apoptosis can stimulate oxidative stress via generation of ROS in cells [Halliwell and Gutteridge, 1990; Chan, 2006; Chan et al., 2006a], suggesting that there is a close relationship between oxidative stress and apoptosis. Nitric oxide (NO) is an important second messenger that is involved in a variety cellular responses and biological functions, including tumor development, metastasis and apoptosis [Rao, 2004; Ekmekcioglu et al., 2005; Zhou and Brune, 2005]. Recent studies have demonstrated that NO is largely produced in mitochondria, through the actions of a Ca^{2+}-sensitive mitochondrial NO synthase (NOS) [Lu et al., 2006; Nazarewicz et al., 2007]. This NOS-mediated NO production could control oxygen consumption and mitochondrial membrane potential through cytochrome *c* oxidase; the NO molecule could then be reactivated with superoxide to produce peroxynitrite, which could further modify its target substrates and induce oxidative stress [Dennis and Bennett, 2003; Brookes, 2004; Ghafourifar and Cadenas, 2005]. Several recent studies have shown that oxidative stress and Ca^{2+} influxes act as upstream regulators for mitochondrial NOS activity [Elfering et al., 2002; Dedkova et al., 2004]. However, the biochemical events involved in MG/HG-induced cell injury and the regulatory mechanisms underlying these effects are still unclear.

Apoptosis and necrosis, two distinct types of cell death, have different biochemical and morphological characteristics and regulatory mechanisms [Majno and Joris, 1995; Schwartz and Bennett, 1995; Chan et al., 2000, 2006b; Chan and Chang, 2006]. Apoptosis plays an important role in the embryogenesis and homeostasis of multicellular organisms, and impairment of apoptotic function has been associated with several human diseases, including neurodegenerative disorders and cancer [Thompson, 1995]. In contrast, necrosis occurs in response to acute and nonphysiological injuries [Alison and Sarraf, 1994]. Recent reports have indicated that the magnitude of the initial insult, not the stimulus type, plays a critical role in prompting a cell to undergo either necrosis or apoptosis [Bonfoco et al., 1995; Hampton and Orrenius, 1997; Chan et al., 2006b]. The 'choice' between necrosis or apoptosis is believed to be controlled by intracellular ATP levels and/or caspase inactivation [Eguchi

et al., 1997]. In particular, high energy levels are required for execution of apoptotic processes, whereas necrosis can proceed in the presence of low ATP levels [Richter et al., 1996; Leist et al., 1997; Chan and Chang, 2006; Chan et al., 2006b]. Here, we focused on examining the effect of ROS and intracellular calcium influxes on NO production, and its modulation effect on cell death modes triggered by combined treatment of human umbilical vein endothelial cells (HUVECs) with MG/HG.

EXPERIMENTAL PROCEDURES

Materials

3-(4, 5-dimethylthiazol-2-yl)-2,5-diphenyltetrazolium bromide (MTT), 2-phenyl-4,4,5,5-tetramethylimidazoline-1-oxyl-3-oxide (PTIO), sodium azide, 2′,7′-dichlorofluorescein diacetate (DCF-DA), propidium iodide, Hoechst 33342, ethyleneglycol-bis(β-aminoethylether)-tetraacetic acid (EGTA) and goat anti-rabbit immunoglobulin G (IgG) antibodies conjugated with alkaline phosphatase were purchased from Sigma (St. Louis, MO). Anti-p53, anti-p21, and anti-β-actin antibodies were from Santa Cruz Biotechnology (Santa Cruz, CA). The monoclonal anti-cytochrome *c* antibody (6H2.B4) was from Imgenex (San Diego, CA). Z-DEVD-AFC was obtained from Calbiochem (La Jolla, CA). The CDP-Star™ chemiluminescent substrate for alkaline phosphatase was acquired from Boehringer Mannheim (Mannheim, Germany).

Cell Culture and Treatment

Human umbilical vein endothelial cell (HUVEC) strain (ECV-304) was obtained from the ATCC, and the cells were cultured at 37°C in a CO_2 incubator in M_{199} medium containing 10% fetal calf serum, with medium changes every 24 h. For experiments, cells (1×10^6) were plated on 60 mm culture dishes, and 24 h later the medium was replaced with medium containing the indicated concentrations of MG and glucose. High glucose treatment was performed by incubating cells in medium containing various concentrations of glucose (5–30 mM) for 24 h. The osmolarity of M_{199} medium (an isotonic solution) was 300 mosmol/kg. Following the addition of 5–30 mM glucose into the medium, the osmolarity of this hypertonic solution was altered to 305–330 mosmol/kg. After 24 h, suspensible cells were collected from cultured medium by centrifugation at 300*g* for 15 min. However, not any cells were collected and found in pellets. This study showed that cells still attached on culture dishes after MG/HG co-treatment for 24 h. The MG/HG co-treated cells were washed twice with ice-cold phosphate-buffered saline (PBS) and lysed on ice for 10 min in 400 μl lysis buffer (20 mM Tris-HCl, pH 7.4, 1 mM EDTA, 1 mM EGTA, 1% Triton X-100, 1 mM benzamidine, 1 mM phenylmethylsulfonyl fluoride, 50 mM NaF, 20 μM sodium pyrophosphate and 1 mM sodium orthovanadate). The cell lysates were sonicated on ice for 3×10 s and centrifuged at 15,000*g* for 20 min at 4°C, and the supernatants were used as cell extracts.

MTT Assay

Cell survival was monitored using the MTT (3-[4,5-dimethylthiazol-2-yl]-2,5-diphenyltetrazolium bromide) test. Briefly, cells were treated with the indicated concentrations of MG and glucose for 24 h, and then treated with 100 μl of 0.45 g/L MTT solution. The cells were incubated at 37°C for 60 min to allow color development, and then 100 μl of 20% SDS in DMF:H_2O (1:1) solution was added to each well to stop the reaction. The plates were incubated overnight at 37°C for solubilization of the formazan products, and spectrophotometric data were measured using an ELISA reader at a wavelength of 570 nm.

Assessment of Necrosis and Apoptosis

Oligonucleosomal DNA fragmentation (a hallmark of apoptosis) was measured using the Cell Death Detection ELISA^{plus} kit (RocheMolecular Biochemicals, Mannheim, Germany). Cells (1×10^5) were treated with or without the indicated concentrations of MG and glucose at 37°C for 24 h, the procedures were performed according to the manufacturer's protocol, and spectrophotometric data were obtained using an ELISA reader at 405 nm. In addition, cells were incubated with propidium iodide (1 μg/ml) and Hoechst 33342 (2 μg/ml) at room temperature for 10 min, and fluorescent microscopy was used to identify the percentage of propidium iodide-impermeable cells having condensed/fragmented nuclei (apoptotic) and the percentage of propidium iodide-permeable cells (necrotic). In each experiment, 7–10 independent fields (~600–1000 nuclei in total) were counted per condition. The activity of lactate

dehydrogenase (LDH) present in the culture medium was evaluated as an additional index of necrosis, as previously described [Behl et al., 1994; Chan and Chang, 2006; Wu and Chan, 2006; Wu and Chan, 2007]. Briefly, cells (5×10^4) were cultured in 96-well microtiter plates (100 μl medium/well), LDH activity was assayed using, and the absorption values at 490 nm were determined with an ELISA reader, according to the manufacturer's instructions (Promega, Madison, WI). Blanks consisted of test substances added to cell-free medium.

ROS Assay

ROS were measured in arbitrary units using 2′,7′-dichlorofluorescein diacetate (DCF-DA) or dihydrorhodamine 123 (DHR 123) dye. Cells (1.0×10^6) were incubated in 50 μl PBS containing 20 μM DCF-DA or DHR123 for 1 h at 37°C, and relative ROS units were determined using a fluorescence ELISA reader (excitation 485 nm, emission 530 nm). An aliquot of the cell suspension was lysed, the protein concentration was determined, and the results were expressed as arbitrary absorbance U/mg protein.

ATP Level Analysis

HUVECs treated with the indicated concentrations of MG and glucose were collected, and ATP levels were quantified with an ATP determination kit. Cells were collected by centrifugation, resuspended in distilled water and then boiled for 5 min. The ATP level in each extract was determined by a bioluminescence assay using a liquid scintillation analyzer, according to the manufacturer's protocol (Molecular Probes, Eugene, OR).

Detection of Intracellular Calcium Concentration ($[Ca^{2+}]i$)

The $[Ca^{2+}]i$ was detected with Fluo-3 AM fluorescence dye, using a modification of the previously reported method [Aoshima et al., 1997; Lu et al., 2006]. Briefly, HUVECs were co-treated with MG and glucose, harvested and washed, and then loaded with 6 μM Fluo-3 AM in standard medium (140 mM NaCl, 5 mM KCl, 1 mM $MgCl_2$, 5.6 mM glucose, 1.5 mM $CaCl_2$, and 20 mM Hepes, pH of 7.4). After 30 min, the cells were washed three times with PBS and then resuspended in standard medium or Ca^{2+}-free standard medium. The fluorescence intensity of Fluo-3 was determined using a fluorescence spectrophotometer (Hitachi, F-2000; excitation at 490 nm, emission at 526 nm).

Detection of Intracellular NO Content

The DAF-2DA fluorescence dye was used to detect intracellular NO, according to a modification of the previously reported method [Nakatsubo et al., 1998; Lu et al., 2006]. Briefly, treated or control cells were collected and washed, and then incubated with 3 μM DAF-2DA. After 60 min, the cells were washed three times with PBS and the fluorescence intensity was measured by a fluorescence spectrophotometer (Hitachi, F-2000; excitation at 485 nm, emission at 515 nm).

Immunoblots

Immunoblotting was performed essentially as described [Chan and Yu, 2000]. Briefly, proteins were separated by SDS–PAGE, following transferred to PVDF membranes, probed with antibodies against cytochrome *c*, caspase-9, caspase-3, eNOS, p53, or p21, respectively and visualized using goat anti-rabbit or anti-mouse IgG antibody conjugated with alkaline phosphatase and CDP-Star™ (chemiluminescent substrate for alkaline phosphatase), according to the manufacturer's protocol (Mannheim, Germany).

Cytochrome *c* Release Assay

Mitochondrial cytochrome *c* release was assayed essentially as described [Yang et al., 1997; Chan et al., 2003]. Cells (1×10^7) were treated with or without the indicated concentrations of MG and glucose, and then harvested by centrifugation (800*g* at 4°C for 15 min). The cells were washed three times with ice-cold PBS, and then resuspended in Hepes buffer (20 mM Hepes, 10 mM KCl, 1.5 mM $MgCl_2$, 1 mM EDTA, 1 mM EGTA, 1 mM DTT, 0.1 mM PMSF, pH 7.5) containing 250 mM sucrose. The suspension was homogenized with a homogenizer, and centrifuged at 800*g* at 4°C for 15 min. The supernatant was centrifuged at 10,000*g* for 15 min at 4°C, and the cytosolic fraction (supernatant) was subjected into 15% SDS–PAGE, transferred to a PVDF membrane and analyzed by immunoblotting with a monoclonal antibody against cytochrome *c*. Immunoreactive bands were detected using an alkaline phosphatase-conjugated goat anti-rabbit IgG antibody and visualized using the CDP-Star™ kit, according

to the manufacturer's protocol (Mannheim, Germany).

Caspase Activity Assays

Caspase-3 activity was measured using the Z-DEVD-AFC fluorogenic substrate, as previously described [Chan et al., 2003; Hsieh et al., 2003]. Caspase-9 activity was assayed using the Colorimetric Caspase-9 Assay Kit (Calbiochem, CA).

Real-Time RT-PCR Assay

Total RNA was extracted with the TRIzol reagent (Life Technologies) and purified with an RNeasy Mini kit (Qiagen), according to the manufacturers' protocols. Real-time PCR was carried out with an ABI 7000 Prism Sequence Detection System (Applied Biosystems). The β-actin mRNA levels were quantified as an endogenous control, and used for normalization. The primers used for PCR were as follows: p53, 5′-CCC ATC CTC ACC ATC ATC AC-3′ and 5′-GTC AGT GGG GAA CAA GAA GTG-3′; p21, 5′-GCC GAA GTC AGT TCC TTG TGG A-3′ and 5′-GTG GGC GGA TTA GGG CTT-3′.

siRNA Knockdown

Lipofectamine was used to transfect HUVECs with 150 nM of siRNA for targeting against p53 (5′-GACUCCAGUGGUAAUCUACTT-3′; sip53), p21 (5′-AACUUCGACUUUGUCACCGAG-3′; coding region 148–168 relative to the start codon), or a scrambled control duplex (5′-GCGCGCUUUGUAGGAUUCG-3′; siScr). Twenty-four hours post-transfection, fresh culture medium was added, and the cells were treated with or without 5 μM MG and 20 mM glucose for another 24 h.

Statistics

Data were analyzed using one-way ANOVA, and differences were evaluated using a two tailed Student's *t*-test and analysis of variance. $P < 0.05$ was considered significant.

RESULTS

Cytotoxic Effects of MG and HG in HUVECs

To examine the combined effects of MG and hyperglycemia, HUVECs were simultaneously treated with MG and HG, and cell viability was examined. Importantly, co-treatment with concentrations of MG and glucose consistent with those observed in plasma from DM patients (5 μM and 15 mM, respectively) could decrease cell viability, whereas treatment with either agent alone did not (Fig. 1A–D). To examine the cell death mode underlying this decreased viability, cells apoptosis and necrosis were measured by TUNEL assay, propidium iodide/Hoechst 33342 staining, and LDH activity assay. Interestingly, HUVECs treated with 5 μM MG and 15–20 mM glucose showed a significant increase in the apoptotic percentage, whereas those treated with 5 μM MG and concentrations of glucose higher than 25 mM showed a significant increase in the necrotic cell population (Fig. 1E–G). These results suggest that co-treatment with MG and HG can cause HUVEC injury through apoptotic and necrotic processes at concentrations similar to those observed in the blood circulation of DM patients.

ROS Generation Increase and ATP Levels Decrease in HUVECs Co-Treated With MG and HG

Since our previous studies demonstrated that numerous stimuli, including MG and HG, can trigger cell apoptosis via ROS generation [Chan, 2005; Hsuuw et al., 2005], we used DCF-DA and DHR 123 to examine whether ROS formation occurred in HUVECs co-treated with MG and HG. Our results showed that 5 μM MG and 15–30 μM HG co-treatment stimulated ROS generation about 8- to 10-fold compared to the untreated control group (Fig. 2A). Interestingly, pretreatment with two commonly-used ROS scavengers, sodium azide and N-acetyl cysteine (NAC), effectively prevented ROS generation triggered by 5 μM MG and 20 mM glucose; moreover it partially blocked by 5 μM MG and 30 mM glucose induction (Fig. 2B). Furthermore, while sodium azide or NAC pretreatment inhibited 5 μM MG/20 mM glucose-induced cell apoptosis, it shifted the mode of 5 μM MG/30 mM glucose-induced cell death from necrosis to apoptosis (Fig. 2C). These results suggest that ROS content could help determine the cell death mode of MG/HG-treated HUVECs.

We previously demonstrated that ATP levels are important mediators capable of switching the mode of cell death from apoptosis to necrosis [Chan et al., 2006b]. To further elucidate the mechanism by which MG/HG triggers either apoptotic or necrotic cell death, we examined the ATP contents in MG/HG-treated HUVECs.

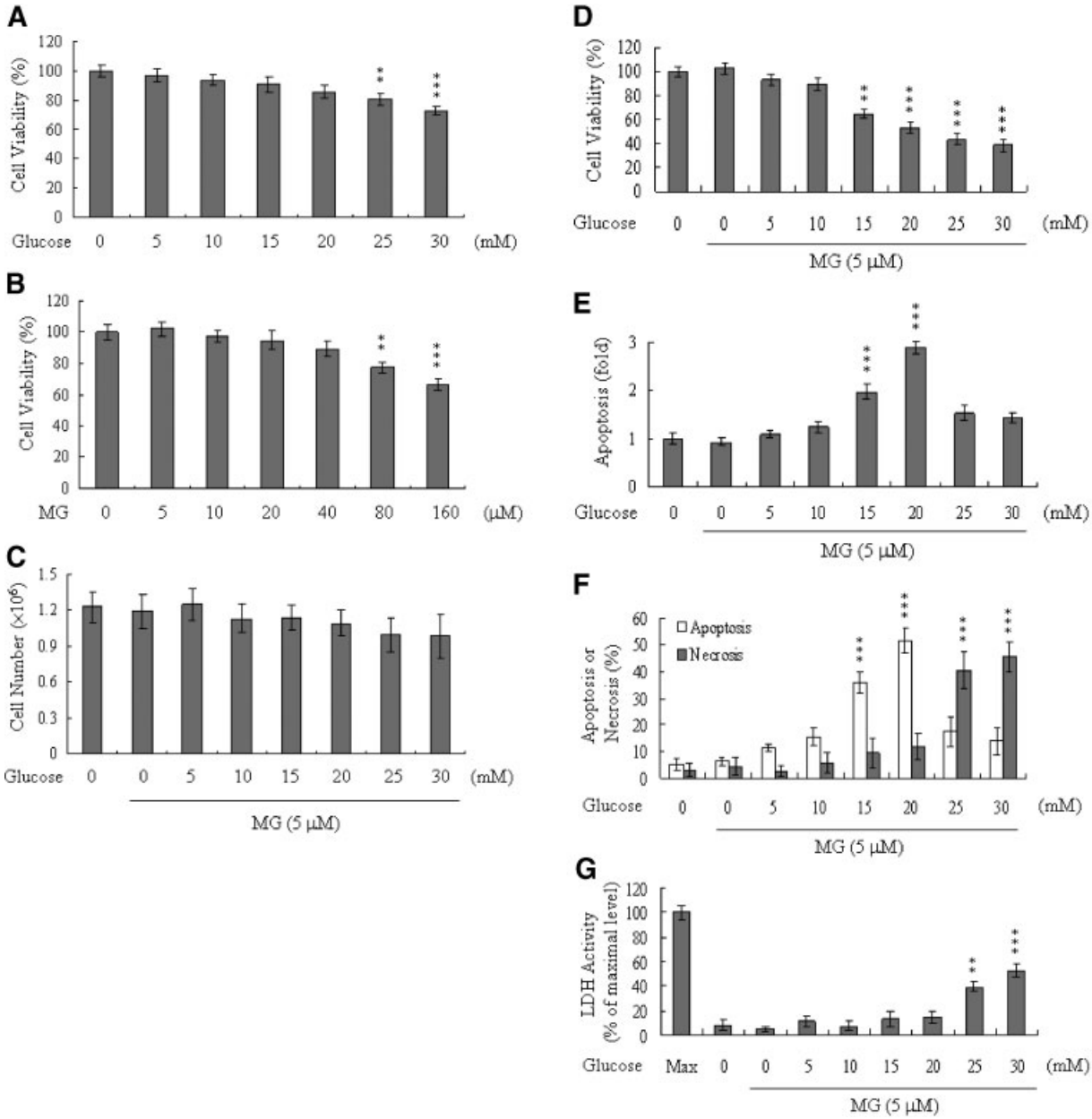

Fig. 1. Effects of MG and HG on HUVECs. **A**,**B**: HUVECs were incubated with 0–30 mM glucose (A) or 0–160 μM MG (B) for 24 h. Cell viability was determined using the MTT assay. **C**–**G**: HUVECs were treated with MG (5 μM) and various concentrations of glucose for 24 h. Total cell numbers after treatment were measured by trypan blue staining (C). Cell viability was measured (D). Cell apoptosis was detected with the Cell Death Detection ELISA kit (E) and staining with propidium iodide and Hoechst 33342 (F). Necrosis was further assessed in terms of LDH activity released in the culture medium, with data expressed as percent of the maximal level (Max) of LDH activity determined after total cell lysis (G). Values are presented as means ± SD of eight determinations. $^{**}P < 0.01$ and $^{***}P < 0.001$ versus the untreated control group.

We found that treatment of HUVECs with 5 μM MG and 25–30 mM glucose triggered decreases in the ATP levels, whereas treatment with 5 μM MG and 5–20 mM glucose had no effect on cellular ATP content (Fig. 3A). To further investigate the role of intracellular ATP levels in MG/HG-induced apoptosis or necrosis, we tested the cell death modes of ATP-depleted cells. HUVECs were treated with and without antimycin (a mitochondrial inhibitor), which was confirmed to cause ATP depletion (Fig. 3B), and we examined the modes of MG/HG-induced cell death. We found that pretreatment of cells with antimycin converted 5 μM MG and 20 mM

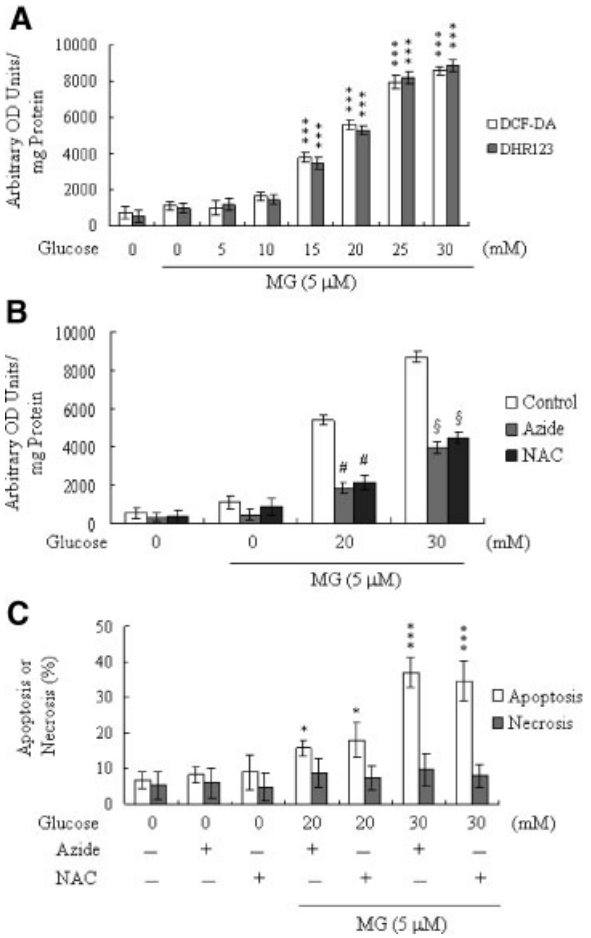

Fig. 2. MG/HG co-treatment appears to evoke oxidative stress in HUVECs. **A**: HUVECs were treated with MG (5 μM) and various concentrations of glucose for 24 h. ROS generation was assayed using DCF-DA (20 μM) or dihydrorhodamine 123 (DHR 123; 20 μM) dye. **B**,**C**: HUVECs were pre-incubated with 2 mM sodium azide or N-acetyl cysteine (NAC; 300 μM) for 30 min and then treated with MG and glucose as indicated. ROS generation was assayed using DCF-DA dye (B). Percentages of apoptosis or necrosis (C) were measured as described in Figure 1. The data are representative of eight independent experiments. $^{*}P < 0.05$ and $^{***}P < 0.001$ versus the un-treated control group. $^{\#}P < 0.001$ versus the ''MG + HG (20 mM)'' group. $^{\S}P < 0.001$ versus the ''MG + HG (30 mM)'' group.

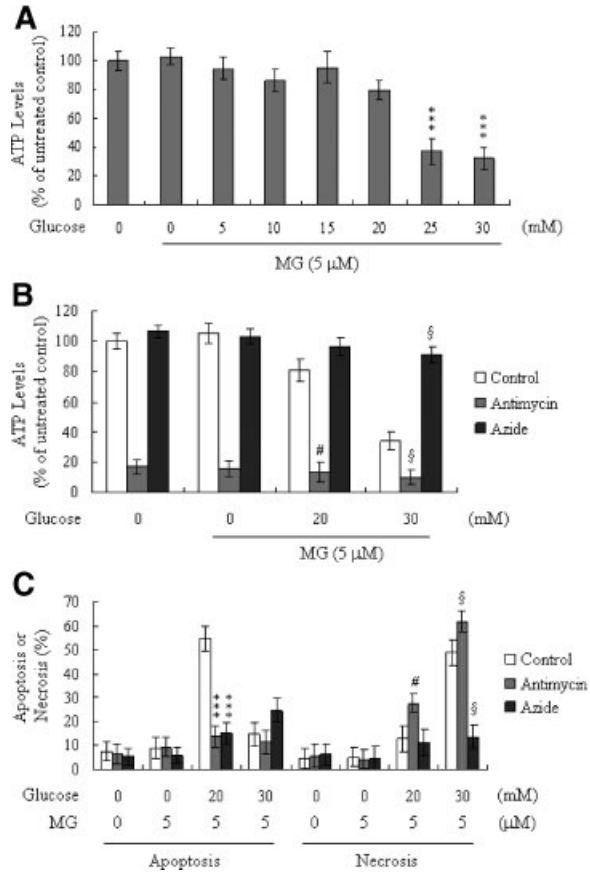

Fig. 3. MG/HG co-treatment appears to induce a decrease in intracellular ATP levels. **A**: HUVECs were treated with MG (5 μM) and various concentrations of glucose for 24 h. Intracellular ATP levels were determined using a bioluminescence-based ELISA assay. The data are given as percent of untreated controls, and the values are presented as the means ± SD of five determinations. **B**,**C**: HUVECs were incubated with antimycin (2 μM) or sodium azide (2 mM) for 1 h and then treated with MG and glucose as indicated for another 24 h. ATP levels (B) and percentage of cell apoptosis or necrosis (C) were measured. The given values are representative of eight determinations. $^{***}P < 0.001$ versus the untreated control group. $^{\#}P < 0.001$ versus the ''MG + HG (20 mM)'' group. $^{\S}P < 0.001$ versus the ''MG + HG (30 mM)'' group.

glucose-induced apoptosis to necrosis, and enhanced 5 μM MG and 30 mM glucose-stimulated necrosis (Fig. 3C). Moreover, sodium azide pretreatment effectively blocked 5 μM MG and 30 mM glucose-induced decreases in ATP levels and induced the subsequent switch from necrosis to apoptosis (Fig. 3B,C), suggesting that ROS content may mediate intracellular ATP levels and modulate the associated switching between apoptosis and necrosis in MG/HG-treated HUVECs.

Changes in Intracellular Ca^{2+} Concentration and NO Levels Are Related to MG/HG-Induced Cell Apoptosis

Changes in $[Ca^{2+}]i$ in MG/HG-treated HUVECs were detected using the Fluo-3 AM fluorescence dye. We found that treatment with 5 μM MG and 20 mM glucose elicited an increase in $[Ca^{2+}]i$, whereas treatment with 5 μM MG and 30 mM glucose did not (Fig. 4A). Furthermore, cells cultured in Ca^{2+}-containing medium showed a ~2-fold increase of $[Ca^{2+}]i$ following treatment with 5 μM MG and 20 mM glucose,

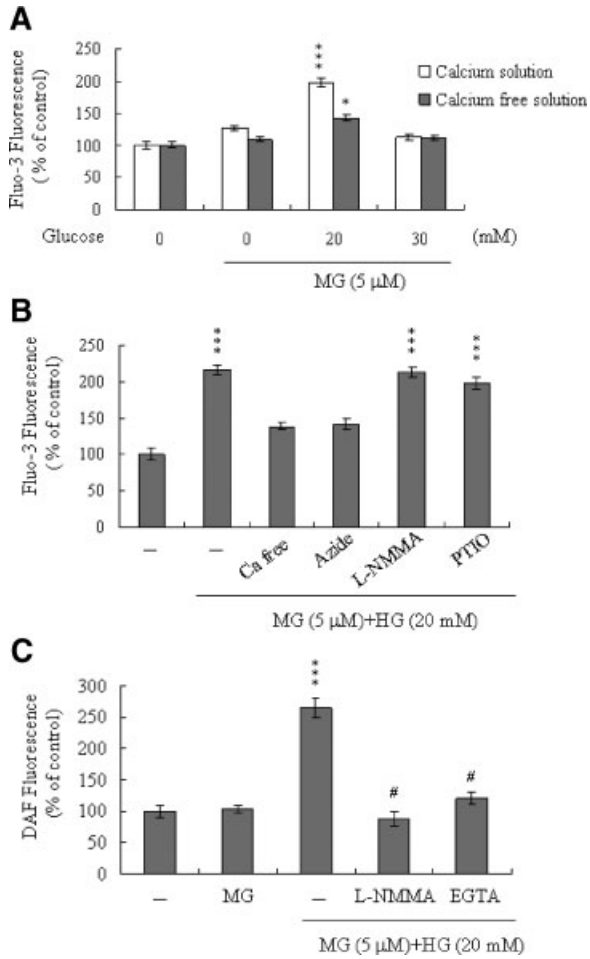

Fig. 4. MG/HG co-treatment triggers changes in intracellular calcium and NO content in HUVECs. **A**: HUVECs were incubated with MG and glucose as indicated for 24 h. Intracellular Fluo-3 fluorescence intensity was measured in the presence/absence of extracellular Ca^{2+}. **B**: We examined the intracellular Ca^{2+} level changes triggered by co-treatment with MG (5 μM) and HG (20 mM), and the effects of ROS and NO inhibitors (Azide: 2 mM; L-NMMA: 0.4 mM; PTIO: 20 μM). **C**: HUVECs were pretreated with L-NMMA (0.4 mM) or EGTA (0.5 mM) for 30 min and then incubated with MG (5 μM) and HG (20 mM). Intracellular NO generation was measured by DAF-2DA fluorescence dye. Data are presented as percentage of control group. $^{*}P < 0.05$ and $^{***}P < 0.001$ versus the untreated control group. $^{\#}P < 0.001$ versus the ''MG + HG'' group.

whereas this increase was largely, but not completely, blocked in treated cells cultured in Ca^{2+}-free cultured medium (Fig. 4A). These findings indicate that the rise in $[Ca^{2+}]$i could be primarily attributed to an influx of external Ca^{2+}, with a smaller portion due to calcium release from intracellular stores, such as those found in the endoplasmic reticulum, mitochondria, nucleus and/or calcium-binding proteins (Fig. 4A).

Our results revealed that PTIO, an inhibitor of NOS and scavenger of NO, and L-NMMA, an inhibitor of NOS, had little effect on 5 μM MG and 20 mM glucose-induced $[Ca^{2+}]$i increases, whereas pretreatment with sodium azide significantly decreased this effect (Fig. 4B). These results suggest that the elevation of $[Ca^{2+}]$i induced by 5 μM MG/20 mM glucose co-treatment may be regulated by ROS generation but not by NO. We further used the NO-sensitive dye, DAF-2DA, to measure intracellular NO generation during MG/HG-induced cell apoptosis. Our results revealed that intracellular NO levels increased in HUVECs co-treated with 5 μM MG and 20 mM glucose (Fig. 4C). However, this increase could be prevented by pretreatment of cells with the NOS inhibitor, L-NMMA (Fig. 4C), or 5 mM EGTA (a Ca^{2+} chelator) (Fig. 4C). These results suggest that intracellular Ca^{2+} levels play an important role in the NOS activation and NO increases observed in HUVECs co-treated with 5 μM MG and 20 mM glucose.

PTIO Inhibits Cytochrome *c* Release and Caspase Activation During MG/HG-Induced Cell Apoptosis

We next analyzed cytochrome *c* release, a major apoptotic event during mitochondrial-mediated apoptotic processes. Cytosolic fractions were isolated from treated and untreated cells, and cytochrome *c* levels were determined by immunoblotting. Significant amounts of cytochrome *c* were released into the cytosol of HUVECs following co-treatment with 5 μM MG and 20 mM glucose, which triggers apoptotic processes, but not following co-treatment with 5 μM MG and 30 mM glucose, which induces necrotic processes (Fig. 5A). In addition, we monitored the activations of caspase-9 and caspase-3, which are known to be involved in cytochrome *c*-mediated apoptosis, and found that co-treatment of HUVECs with 5 μM MG and 20 mM glucose stimulated the cleavage/activation of caspase-9 (Fig. 5A,B) and caspase-3 (Fig. 5A,C), whereas co-treatment with 5 μM MG and 30 mM glucose failed to. Importantly, both caspases activation and the release of cytochrome *c* from mitochondria into the cytosol were significantly inhibited by incubation of cells with 20 μM PTIO prior to co-treatment with 5 μM MG and 20 mM glucose (Fig. 5A–C). These results indicate that increases in NO level may act as an upstream regulator for

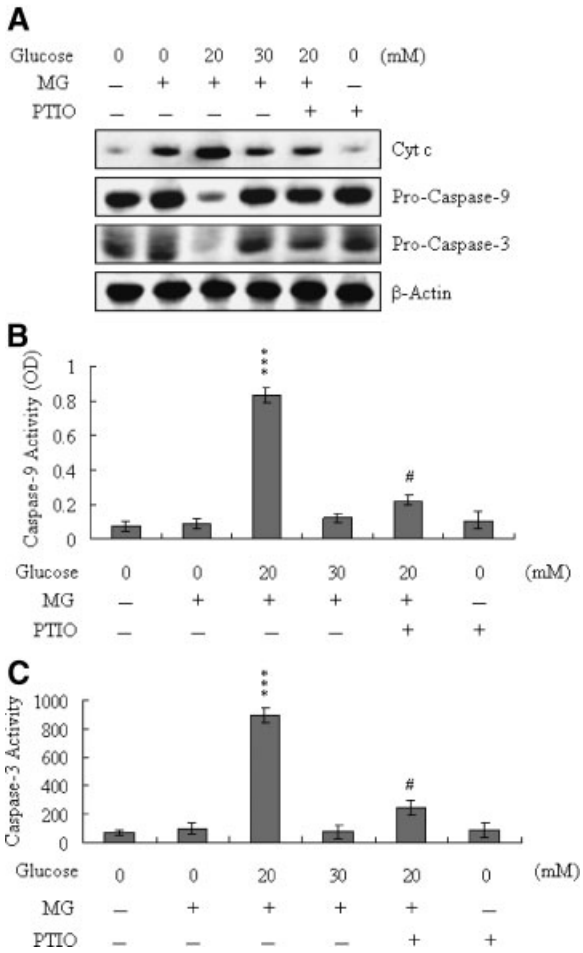

Fig. 5. Cytochrome *c* release and activation of caspase-9 and -3 by MG/HG treatment of HUVECs. HUVECs were pretreated with PTIO (20 μM) for 1 h and then treated with MG (5 μM) and the indicated concentrations of glucose for another 24 h. **A**: Cytosolic fractions were separated and then immunoblotted with antibodies against cytochrome *c* (Cyt *c*), pro-caspase-9 and pro-caspase-3. **B**: Caspase-9 activities were assayed using the Colorimetric Caspase-9 Assay kit. **C**: Caspase-3 activities were analyzed using Z-DEVD-AFC as the substrate. $^{***}P < 0.001$ versus the untreated control group. $^{\#}P < 0.001$ versus the "MG + HG (20 mM)" group.

cytochrome *c* release and activation of caspase-9 and -3 during the MG/HG-induced apoptosis, but not necrosis, of HUVECs.

Changes of mRNA and Protein Expression Levels Following MG/HG-Treatment of HUVECs

The results from our real-time RT-PCR and immunoblotting analyses showed that endothelial cell nitric oxide synthase (eNOS), p53 and p21 were significantly up-regulated at the mRNA and protein levels in HUVECs co-treated with 5 μM MG and 20 mM glucose, but these changes could be blocked by pretreatment with sodium azide or PTIO (Fig. 6A–D).

Inhibition of p53 and p21 by siRNA Knockdown Blocks MG/HG-Induced Apoptosis in HUVECs

To further determine the role of p53 and p21 in MG/HG-induced apoptosis, we used targeted siRNAs to decrease the expression levels of p53 and p21 in HUVECs, and then incubated the cells with 5 μM MG and 20 mM glucose for 24 h and tested for cell viability. The siRNA knockdown significantly decreased the protein levels of p53 and p21 in MG/HG-treated HUVECs (Fig. 7A,B), and this decrease in p53 or p21 protein expression was associated with a significant decrease in MG/HG-induced apoptosis (Fig. 7C). These results suggest that MG/HG treatment up-regulates p53 and p21 in HUVECs, and this effect is involved in subsequent apoptosis of the treated cells.

DISCUSSION

Increased concentrations of MG and glucose in blood are two major symptoms of DM. We previously showed that treatment with glucose at concentrations higher than 25 mM could induce apoptotic processes in the K562 human leukemia cell line [Chan, 2005], and that 250 μM MG caused various cells injuries, including apoptosis [Hsuuw et al., 2005]. Our present results indicate that glucose alone at concentrations higher than 25 mM or MG alone at concentrations higher than 80 μM could decrease cell viability in HUVEC (Fig. 1A,B). However, the physiological concentrations of glucose and MG found in the blood of DM patients are more on the order of 20–30 mM glucose and 5–6 μM MG [McLellan et al., 1994]. Thus, the cytotoxicity effects of MG and HG alone occur at treatment doses much higher than those seen in DM patients (Fig. 1A,B), and no injury effects are seen in HUVECs exposed to physiologically relevant concentrations of glucose or MG alone (Fig. 1A,B). However, since hyperglycemia and increased MG levels are seen simultaneously in DM patients, we herein investigated the effects of co-treatment with physiologically relevant concentrations of MG and glucose. Our results revealed that co-treatment of HUVECs with 5 μM MG and 15–30 mM HG could significantly decrease cell viability (Fig. 1D). Furthermore, we found that within this range, the glucose concentration

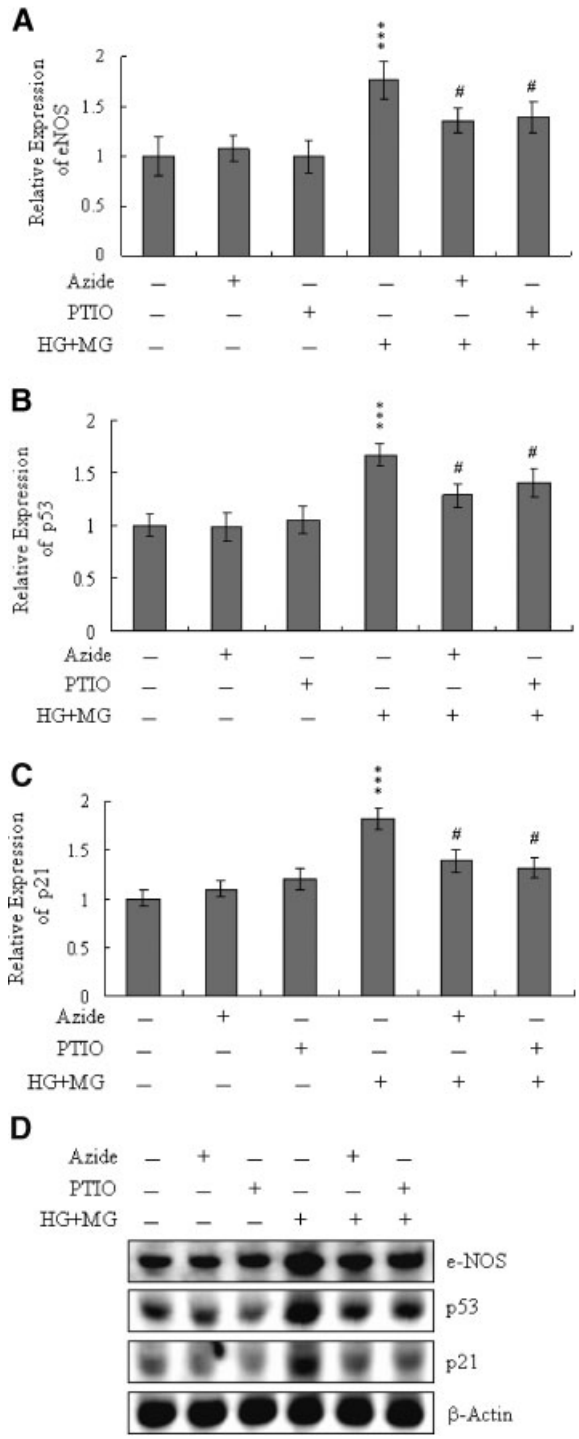

Fig. 6. Effect of sodium azide and PTIO on the mRNA and protein expression levels of eNOS, p53 and p21. HUVECs were pre-incubated with or without sodium azide (2 mM) and PTIO (20 μM) for 1 h and then treated with MG (5 μM) and HG (20 mM) for another 24 h. The mRNA expression levels of eNOS (**A**), p53 (**B**) and p21 (**C**) were analyzed using real-time PCR. **D**: The protein expression levels of eNOS, p53, and p21 were detected by immunoblotting. The given values are representative of eight determinations. $^{***}P < 0.001$ versus the untreated control group. $^{\#}P < 0.001$ versus the ''MG + HG'' group.

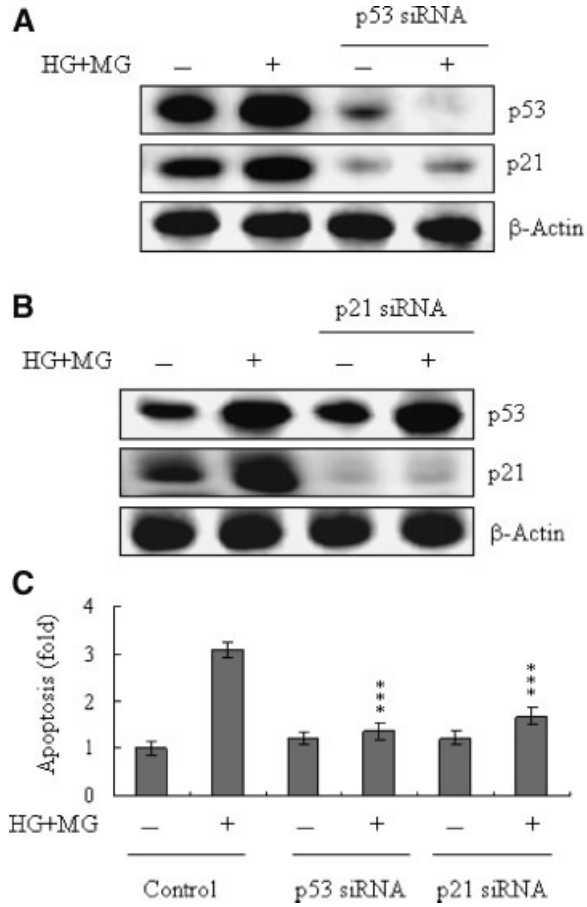

Fig. 7. Knockdown of p53 and p21 can protect HUVECs against MG/HG-induced apoptosis. HUVECs were transfected with siRNA targeting p53 or p21, incubated for 24 h, and then treated with MG (5 μM) and HG (20 mM) for another 24 h. Cell extracts were analyzed by immunoblotting using antibodies against p53 (**A**), p21 (**B**) and β-actin. **C**: Cell apoptosis was measured as described in Figure 1. $^{***}P < 0.001$ versus the ''MG + HG'' group.

could determine whether cell death occurred via apoptosis or necrosis (Fig. 1E–G).

Earlier studies demonstrated that HG increases ROS generation in human aortic endothelial cells [Cosentino et al., 1997] and K562 cells [Chan, 2005], and triggers apoptosis in HUVEC cells [Baumgartner-Parzer et al., 1995]. In addition, a recent study showed that intracellular ROS was generated by MG treatment of mouse embryonic stem cells [Hsuuw et al., 2005]. Several mechanisms have been proposed to explain the generation of ROS following MG treatment. For example, MG could mediate glycation reactions with amino acids or proteins, MG metabolism could deplete the glutathione content of cells, and/or MG may modify or inactivate ROS scavenger enzymes [Yim et al., 1995; Lee et al., 1998; Oya et al., 1999]. The

present study showed that in cells treated with 5 μM MG, co-treatment with concentrations of glucose higher than 15 mM significantly increased ROS generation (Fig. 2A), and the ROS content in these cells helped determine whether subsequent cell death proceeded through apoptosis or necrosis (Fig. 2C). These results demonstrated that physiologically relevant concentrations of MG and glucose comparable to those found in the blood of DM patients could synergistically cooperate to evoke ROS generation and induce cell apoptosis or necrosis.

Chemically induced hypoxia has been shown to activate several distinct cell death types, depending on the intensity of the stimulus or triggering insult in rat fibroblastic cells [Formigli et al., 2000]. Apoptosis predominated in cells treated with low doses of antimycin A, a specific inhibitor of the mitochondrial respiratory chain, while necrosis was increasingly favored as the intensity of the hypoxic insult increased [Formigli et al., 2000]. Other studies have suggested that intracellular ATP levels could represent an important regulator for switching cells toward apoptosis or necrosis [Richter et al., 1996; Eguchi et al., 1997; Formigli et al., 2000; Chan et al., 2006b], with necrosis favored under low ATP conditions in many model systems. Consistent with this notion, studies have shown that high ATP levels are essential for the nuclear morphologic changes characteristic of apoptosis [Kass et al., 1996]. We previously showed that 50–200 and 12.5–25 μM curcumin induced two distinct cell death programs in osteoblasts; in this system curcumin dose-dependently decreased the intracellular ATP levels in osteoblasts, and this ATP depletion could effectively switch curcumin-induced apoptosis to necrosis [Chan et al., 2006b]. In the present work, we found that the ROS content of MG/HG-treated HUVECs could affect the intracellular ATP levels and help determine the mode of the induced cell death (Fig. 3). Based on the previous reports and our present results, we propose that ROS content and ATP level can act as the switch for determining whether MG/HG-induced cell death in HUVECs proceeds through apoptosis or necrosis.

Previous studies have shown that increases in intracellular calcium levels can play an important role in regulating cell death [Inanami et al., 1999; Almeida et al., 2004; Lu et al., 2006]. In this study, we elucidated whether MG/HG treatment induced cell apoptosis through intracellular calcium increases. We observed increases in $[Ca^{2+}]i$ following MG/HG treatment, and found that this increase in $[Ca^{2+}]i$ was largely due to an influx of Ca^{2+} from the extracellular medium (Fig. 4A,B). This effect could be significantly blocked by sodium azide (Fig. 4B), indicating that MG/HG-induced ROS generation is responsible for the elevation of intracellular calcium concentrations in MG/HG-treated HUVECs.

NO is an endogenously product from NADPH, O_2 and L-arginine catalyzed by nitric oxide synthase. A recent study demonstrated that NO production was involved in apoptosis triggered by several different types of stimuli [Lu et al., 2006; Nazarewicz et al., 2007]. The regulatory actions of NO on the mitochondrial apoptotic signaling pathways are well documented. Decreased ratios of Bcl-2/Bax and inhibition of the electron transport are regulatory mechanisms of NO-mediated apoptosis [Monteiro et al., 2004]. Decrease on Bcl-2/Bax ratios and impairment of mitochondrial electron transport may cause release of cytochrome *c* which involved in the control of cell apoptosis. In addition, tamoxifen treatment increased intramitochondrial Ca^{2+} concentrations, leading to stimulation of mitochondrial NO synthase activity and enhancement of NO production in rat livers and human breast cancer MCF-7 cells [Nazarewicz et al., 2007]. Here, we observed NO generation following MG/HG treatment of HUVECs, with intracellular NO levels ~2.5-fold higher in treated cells versus untreated controls (Fig. 4C). Pretreatment with EGTA in the extracellular medium significantly prevented this increase in intracellular NO (Fig. 4C), indicating that NO production in MG/HG-treated HUVECs is dependent on the intracellular calcium concentration. Furthermore, consistent with the notion that NOS is the main source of NO production during stimulus-triggered apoptosis [Lu et al., 2006; Nazarewicz et al., 2007], we found that the mRNA and protein expression levels of eNOS were ~1.8-fold higher in MG/HG-treated HUVECs versus untreated controls (Fig. 6A). The regulatory role of NO in cell apoptosis is very complex, and studies have shown that NO-mediated apoptotic effects are modulated by different mechanisms in different cell types [Rao, 2004; Li and Wogan, 2005]. A previous study showed that NOS substrates or NO donors could inhibit

photodynamic treatment-induced apoptosis in CCRF-CEM cells [Gomes et al., 2002]. Here, we found that PTIO treatment attenuated cytochrome *c* release and decreased caspases activation (Fig. 5), suggesting that NO generation may be an important mediator of apoptosis in MG/HG-treated HUVECs.

It is well known that NO-mediated apoptotic processes are associated with p53 gene activation, which is essential for regulation of cell cycle and/or apoptotic signaling occurring through $p21^{Waf1/Cip1}$ or Bax [Li et al., 2004; Okada and Mak, 2004]. In this study, we found that both p53 and p21 mRNA levels were up-regulated by treatment with MG/HG, and this up-regulation was blocked by pretreatment with PTIO (Fig. 6). Furthermore, siRNA-mediated knockdown of p53 protein expression prevented MG/HG-induced increases in the protein levels of p21, and decreased subsequent apoptosis, whereas p21 knockdown blocked MG/HG-triggered apoptosis in HUVECs but had no effect on the expression of p53 (Fig. 7A–C). These results indicate that the genes encoding p53 and p21 are activated during MG/HG-induced apoptosis of HUVECs, and further suggest that NO plays an important role in regulating gene expression and cell death in MG/HG-treated HUVECs.

Based on the results of the present study, we propose the following model of MG/HG-induced cell injury signaling in HUVECs (Fig. 8). Co-treatment of cells with MG and HG directly evoke ROS generation, with the treatment dosage affecting the amount of generated ROS. The ROS content determines intracellular ATP levels, and these levels regulate the cell death, with high ATP levels favoring apoptosis and low ATP levels favoring necrosis. In addition, high levels of intracellular ROS trigger an influx of calcium from the extracellular medium, leading to increased intracellular calcium concentrations, which activate NOS and induce generation of NO. Pretreatment with sodium azide or PTIO can block the MG/HG-induced up-regulation of critical genes/proteins and rescue cell viability. Thus, our results collectively show that both intracellular ROS and NO play critical roles in MG/HG-induced cell apoptosis of HUVECs.

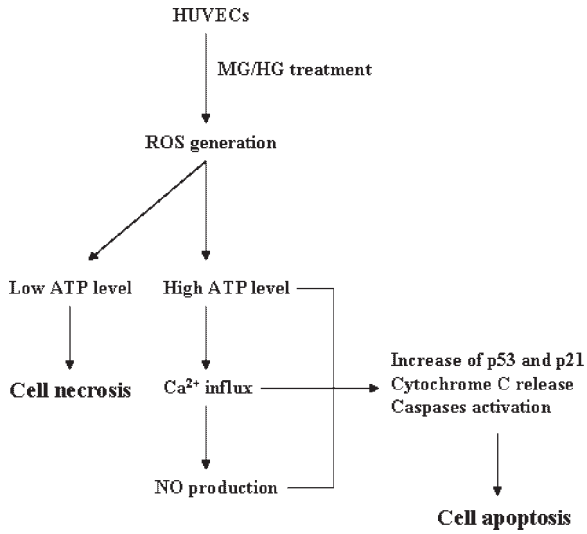

Fig. 8. Scheme of events occurring during MG/HG-induced cell death in HUVECs.

ACKNOWLEDGMENTS

This work was supported by grants (NSC 95-2311-B-033-001-MY3 and NSC 95-2627-M-033-004) from the National Science Council of Taiwan, ROC, and from the Center-of-Excellence Program on Membrane Technology, Ministry of Education, Taiwan, ROC.

REFERENCES

Alison MR, Sarraf CE. 1994. Liver cell death: Patterns and mechanisms. Gut 35:577–581.

Almeida RD, Manadas BJ, Carvalho AP, Duarte CB. 2004. Intracellular signaling mechanisms in photodynamic therapy. Biochim Biophys Acta 1704:59–86.

Aoshima H, Satoh T, Sakai N, Yamada M, Enokido Y, Ikeuchi T, Hatanaka H. 1997. Generation of free radicals during lipid hydroperoxide-triggered apoptosis in PC12h cells. Biochim Biophys Acta 1345:35–42.

Baumgartner-Parzer SM, Wagner L, Pettermann M, Grillari J, Gessl A, Waldhausl W. 1995. High-glucose—Triggered apoptosis in cultured endothelial cells. Diabetes 44:1323–1327.

Behl C, Davis JB, Lesley R, Schubert D. 1994. Hydrogen peroxide mediates amyloid beta protein toxicity. Cell 77:817–827.

Bonfoco E, Krainc D, Ankarcrona M, Nicotera P, Lipton SA. 1995. Apoptosis and necrosis: Two distinct events induced, respectively, by mild and intense insults with N-methyl-D-aspartate or nitric oxide/superoxide in cortical cell cultures. Proc Natl Acad Sci USA 92:7162–7166.

Bourajjaj M, Stehouwer CD, van Hinsbergh VW, Schalkwijk CG. 2003. Role of methylglyoxal adducts in the development of vascular complications in diabetes mellitus. Biochem Soc Trans 31:1400–1402.

Brookes PS. 2004. Mitochondrial nitric oxide synthase. Mitochondrion 3:187–204.

Brownlee M, Cerami A, Vlassara H. 1988. Advanced glycosylation end products in tissue and the biochemical basis of diabetic complications. N Engl J Med 318:1315–1321.

Chan WH. 2005. Effect of resveratrol on high glucose-induced stress in human leukemia K562 cells. J Cell Biochem 94:1267–1279.

Chan WH. 2006. Ginkgolide B induces apoptosis and developmental injury in mouse embryonic stem cells and blastocysts. Hum Reprod 21:2985–2995.

Chan WH, Chang YJ. 2006. Dosage effects of resveratrol on ethanol-induced cell death in the human K562 cell line. Toxicol Lett 161:1–9.

Chan WH, Wu HJ. 2006. Protective effects of curcumin on methylglyoxal-induced oxidative DNA damage and cell injury in human mononuclear cells. Acta Pharmacol Sin 27:1192–1198.

Chan WH, Yu JS. 2000. Inhibition of UV irradiation-induced oxidative stress and apoptotic biochemical changes in human epidermal carcinoma A431 cells by genistein. J Cell Biochem 78:73–84.

Chan WH, Yu JS, Yang SD. 1999. PAK2 is cleaved and activated during hyperosmotic shock-induced apoptosis via a caspase-dependent mechanism: Evidence for the involvement of oxidative stress. J Cell Physiol 178:397–408.

Chan WH, Yu JS, Yang SD. 2000. Apoptotic signalling cascade in photosensitized human epidermal carcinoma A431 cells: Involvement of singlet oxygen, c-Jun N-terminal kinase, caspase-3 and p21-activated kinase 2. Biochem J 351:221–232.

Chan WH, Wu CC, Yu JS. 2003. Curcumin inhibits UV irradiation-induced oxidative stress and apoptotic biochemical changes in human epidermoid carcinoma A431 cells. J Cell Biochem 90:327–338.

Chan WH, Wu HJ, Hsuuw YD. 2005. Curcumin inhibits ROS formation and apoptosis in methylglyoxal-treated human hepatoma G2 cells. Ann N Y Acad Sci 1042:372–378.

Chan WH, Shiao NH, Lu PZ. 2006a. CdSe quantum dots induce apoptosis in human neuroblastoma cells via mitochondrial-dependent pathways and inhibition of survival signals. Toxicol Lett 167:191–200.

Chan WH, Wu HY, Chang WH. 2006b. Dosage effects of curcumin on cell death types in a human osteoblast cell line. Food Chem Toxicol 44:1362–1371.

Cosentino F, Hishikawa K, Katusic ZS, Luscher TF. 1997. High glucose increases nitric oxide synthase expression and superoxide anion generation in human aortic endothelial cells. Circulation 96:25–28.

Dedkova EN, Ji X, Lipsius SL, Blatter LA. 2004. Mitochondrial calcium uptake stimulates nitric oxide production in mitochondria of bovine vascular endothelial cells. Am J Physiol Cell Physiol 286:C406–C415.

Dennis J, Bennett JP Jr. 2003. Interactions among nitric oxide and Bcl-family proteins after MPP+ exposure of SH-SY5Y neural cells I: MPP+ increases mitochondrial NO and Bax protein. J Neurosci Res 72: 76–88.

Eguchi Y, Shimizu S, Tsujimoto Y. 1997. Intracellular ATP levels determine cell death fate by apoptosis or necrosis. Cancer Res 57:1835–1840.

Ekmekcioglu S, Tang CH, Grimm EA. 2005. NO news is not necessarily good news in cancer. Curr Cancer Drug Targets 5:103–115.

Elfering SL, Sarkela TM, Giulivi C. 2002. Biochemistry of mitochondrial nitric-oxide synthase. J Biol Chem 277: 38079–38086.

Formigli L, Papucci L, Tani A, Schiavone N, Tempestini A, Orlandini GE, Capaccioli S, Orlandini SZ. 2000. Aponecrosis: Morphological and biochemical exploration of a syncretic process of cell death sharing apoptosis and necrosis. J Cell Physiol 182:41–49.

Gerozissis K. 2003. Brain insulin: Regulation, mechanisms of action and functions. Cell Mol Neurobiol 23:1–25.

Ghafourifar P, Cadenas E. 2005. Mitochondrial nitric oxide synthase. Trends Pharmacol Sci 26:190–195.

Gomes ER, Almeida RD, Carvalho AP, Duarte CB. 2002. Nitric oxide modulates tumor cell death induced by photodynamic therapy through a cGMP-dependent mechanism. Photochem Photobiol 76:423–430.

Halliwell B, Gutteridge JM. 1990. Role of free radicals and catalytic metal ions in human disease: An overview. Methods Enzymol 186:1–85.

Hampton MB, Orrenius S. 1997. Dual regulation of caspase activity by hydrogen peroxide: Implications for apoptosis. FEBS Lett 414:552–556.

Ho FM, Liu SH, Liau CS, Huang PJ, Lin-Shiau SY. 2000. High glucose-induced apoptosis in human endothelial cells is mediated by sequential activations of c-Jun NH(2)-terminal kinase and caspase-3. Circulation 101: 2618–2624.

Hsieh YJ, Wu CC, Chang CJ, Yu JS. 2003. Subcellular localization of Photofrin determines the death phenotype of human epidermoid carcinoma A431 cells triggered by photodynamic therapy: When plasma membranes are the main targets. J Cell Physiol 194:363–375.

Hsuuw YD, Chang CK, Chan WH, Yu JS. 2005. Curcumin prevents methylglyoxal-induced oxidative stress and apoptosis in mouse embryonic stem cells and blastocysts. J Cell Physiol 205:379–386.

Inanami O, Yoshito A, Takahashi K, Hiraoka W, Kuwabara M. 1999. Effects of BAPTA-AM and forskolin on apoptosis and cytochrome c release in photosensitized Chinese hamster V79 cells. Photochem Photobiol 70:650–655.

Jan CR, Chen CH, Wang SC, Kuo SY. 2005. Effect of methylglyoxal on intracellular calcium levels and viability in renal tubular cells. Cell Signal 17:847–855.

Kasai H, Kumeno K, Yamaizumi Z, Nishimura S, Nagao M, Fujita Y, Sugimura T, Nukaya H, Kosuge T. 1982. Mutagenicity of methylglyoxal in coffee. Gann 73:681–683.

Kass GE, Eriksson JE, Weis M, Orrenius S, Chow SC. 1996. Chromatin condensation during apoptosis requires ATP. Biochem J 318(Pt 3):749–752.

Lee C, Yim MB, Chock PB, Yim HS, Kang SO. 1998. Oxidation-reduction properties of methylglyoxal-modified protein in relation to free radical generation. J Biol Chem 273:25272–25278.

Leist M, Single B, Castoldi AF, Kuhnle S, Nicotera P. 1997. Intracellular adenosine triphosphate (ATP) concentration: A switch in the decision between apoptosis and necrosis. J Exp Med 185:1481–1486.

Li CQ, Wogan GN. 2005. Nitric oxide as a modulator of apoptosis. Cancer Lett 226:1–15.

Li CQ, Robles AI, Hanigan CL, Hofseth LJ, Trudel LJ, Harris CC, Wogan GN. 2004. Apoptotic signaling pathways induced by nitric oxide in human lymphoblastoid cells expressing wild-type or mutant p53. Cancer Res 64:3022–3029.

Lu Z, Tao Y, Zhou Z, Zhang J, Li C, Ou L, Zhao B. 2006. Mitochondrial reactive oxygen species and nitric oxide-mediated cancer cell apoptosis in 2-butylamino-2-

demethoxyhypocrellin B photodynamic treatment. Free Radic Biol Med 41:1590–1605.
Majno G, Joris I. 1995. Apoptosis, oncosis, and necrosis. An overview of cell death. Am J Pathol 146:3–15.
McLellan AC, Thornalley PJ, Benn J, Sonksen PH. 1994. Glyoxalase system in clinical diabetes mellitus and correlation with diabetic complications. Clin Sci (Lond) 87:21–29.
Messier C, Gagnon M. 1996. Glucose regulation and cognitive functions: Relation to Alzheimer's disease and diabetes. Behav Brain Res 75:1–11.
Monteiro HP, Silva EF, Stern A. 2004. Nitric oxide: A potential inducer of adhesion-related apoptosis—Anoikis. Nitric Oxide 10:1–10.
Nakatsubo N, Kojima H, Kikuchi K, Nagoshi H, Hirata Y, Maeda D, Imai Y, Irimura T, Nagano T. 1998. Direct evidence of nitric oxide production from bovine aortic endothelial cells using new fluorescence indicators: Diaminofluoresceins. FEBS Lett 427:263–266.
Nazarewicz RR, Zenebe WJ, Parihar A, Larson SK, Alidema E, Choi J, Ghafourifar P. 2007. Tamoxifen induces oxidative stress and mitochondrial apoptosis via stimulating mitochondrial nitric oxide synthase. Cancer Res 67:1282–1290.
Okada H, Mak TW. 2004. Pathways of apoptotic and non-apoptotic death in tumour cells. Nat Rev Cancer 4:592–603.
Okado A, Kawasaki Y, Hasuike Y, Takahashi M, Teshima T, Fujii J, Taniguchi N. 1996. Induction of apoptotic cell death by methylglyoxal and 3-deoxyglucosone in macrophage-derived cell lines. Biochem Biophys Res Commun 225:219–224.
Okouchi M, Okayama N, Aw TY. 2005. Hyperglycemia potentiates carbonyl stress-induced apoptosis in naive PC-12 cells: Relationship to cellular redox and activator protease factor-1 expression. Curr Neurovasc Res 2:375–386.
Ota K, Nakamura J, Li W, Kozakae M, Watarai A, Nakamura N, Yasuda Y, Nakashima E, Naruse K, Watabe K, Kato K, Oiso Y, Hamada Y. 2007. Metformin prevents methylglyoxal-induced apoptosis of mouse Schwann cells. Biochem Biophys Res Commun 357: 270–275.
Oya T, Hattori N, Mizuno Y, Miyata S, Maeda S, Osawa T, Uchida K. 1999. Methylglyoxal modification of protein. Chemical and immunochemical characterization of methylglyoxal-arginine adducts. J Biol Chem 274: 18492–18502.
Qin S, Minami Y, Kurosaki T, Yamamura H. 1997. Distinctive functions of Syk and Lyn in mediating osmotic stress- and ultraviolet C irradiation-induced apoptosis in chicken B cells. J Biol Chem 272:17994–17999.
Rao CV. 2004. Nitric oxide signaling in colon cancer chemoprevention. Mutat Res 555:107–119.
Richter C, Schweizer M, Cossarizza A, Franceschi C. 1996. Control of apoptosis by the cellular ATP level. FEBS Lett 378:107–110.
Schwartz SM, Bennett MR. 1995. Death by any other name. Am J Pathol 147:229–234.
Shipanova IN, Glomb MA, Nagaraj RH. 1997. Protein modification by methylglyoxal: Chemical nature and synthetic mechanism of a major fluorescent adduct. Arch Biochem Biophys 344:29–36.
Thompson CB. 1995. Apoptosis in the pathogenesis and treatment of disease. Science 267:1456–1462.
Uchida K, Khor OT, Oya T, Osawa T, Yasuda Y, Miyata T. 1997. Protein modification by a Maillard reaction intermediate methylglyoxal. Immunochemical detection of fluorescent 5-methylimidazolone derivatives in vivo. FEBS Lett 410:313–318.
Wu HJ, Chan WH. 2007. Genistein protects methylglyoxal-induced oxidative DNA damage and cell injury in human mononuclear cells. Toxicol In Vitro 21:335–342.
Yang J, Liu X, Bhalla K, Kim CN, Ibrado AM, Cai J, Peng TI, Jones DP, Wang X. 1997. Prevention of apoptosis by Bcl-2: Release of cytochrome c from mitochondria blocked. Science 275:1129–1132.
Yim HS, Kang SO, Hah YC, Chock PB, Yim MB. 1995. Free radicals generated during the glycation reaction of amino acids by methylglyoxal. A model study of protein-cross-linked free radicals. J Biol Chem 270:28228–28233.
Zhou J, Brune B. 2005. NO and transcriptional regulation: From signaling to death. Toxicology 208:223–233.